Study of catastrophic dechannelling resonance in strained layer superlattices using a shell structure potential

1995 J. Phys.: Condens. Matter 7 7805

(http://iopscience.iop.org/0953-8984/7/40/011)

J. Phys.: Condens. Matter 7 (1995) 7805–7812. Printed in the UK

Study of catastrophic dechannelling resonance in strained layer superlattices using a shell structure potential

V Hari Kumar and A P Pathak

School of Physics, University of Hyderabad, Central University PO, Hyderabad 500 046, India

Received 11 November 1994, in final form 7 August 1995

Abstract. Catastrophic dechannelling resonance (CDR) occurs when the half wavelength ($\lambda/2$) of a planar channelled ion beam matches the path length per layer, s, of a strained layer superlattice (SLS). CDR has been used for probing important properties of SLS. The dependence of CDR on various parameters, like incident angle, minimum impact parameter for channelling and superlattice strain in strained layer superlattices, are studied using a shell structure potential, which is based on the atomic shell structure of the target (SLS) atom. We have taken a $GaAs_{0.09}P_{0.91}/GaP$ ($s = 48.2$ nm) superlattice as our target and a ^4He ion beam as the incident probe beam. Comparison with other frequently used Thomas–Fermi-type potentials and good agreement with experimental results shows the usefulness and accuracy of this shell model potential.

1. Introduction

Strained layer superlattices (SLS) are layered structures of alternating composition of materials having a not too large (~0.1–2.0%) lattice mismatch [1,2]. This small lattice mismatch is accommodated by biaxial (compressive and tensile) strains in the plane of the layers and each layer acquires a perpendicular lattice constant due to strain accommodation. Thus for sufficiently thin layers misfit defects or dislocations are not generated. Due to these alternating tetragonal distortions along the growth direction, inclined crystal planes and rows undergo abrupt tilt ($\Delta\psi$) at each interface [3].

The unusual electronic and optoelectronic properties of SLS have opened up a new category of electronic and optoelectronic devices, which have wide-ranging applications in many frontier areas of science and technology. The ability to tailor the energy band gap in SLS is one of the properties which is utilized in the manufacture of photodetectors and quantum well lasers. The presence of defects deteriorates the performance of these semiconductor devices, so it is important to characterize strain and strain-relief mechanisms in the structures. Rutherford back-scattering analysis, along with channelling [4] measurements, are extensively used for this purpose. Since channelled particles do not approach the atomic nuclei, a substantial reduction in the scattering yield occurs whenever a particle is channelled. The presence of misfit defects or dislocations and the changes in the direction of the crystal rows or planes at the interfaces will give rise to dechannelling due to scattering. Catastrophic dechannelling resonance occurs when the half wavelength ($\lambda/2$) of oscillatory motion of a planar channelled ion beam matches the path length per layer (s) of the SLS. Study of this resonance gives information on the strains present in SLS. Charged-particle (α particle) channelling along the inclined (110) crystal plane of a $GaAs_{0.09}P_{0.91}/GaP$ superlattice under conditions of catastrophic dechannelling

0953-8984/95/407805+08$19.50

has been reported elsewhere [3,5–8]. A Moliere planar potential based on the Thomas–Fermi model [9] has mostly been used in these studies. Here we have used a shell model potential [10], which is free from the statistical nature of the Moliere potential and takes into account the detailed atomic shell structure of the target material (SLS).

Earlier we successfully used the same shell model charged density and shell potential for various other problems, like stopping power, channelling radiation etc, in the related problems of ion channelling studies [10–12]. This provided us with motivation to use this shell model potential in the exciting field of SLS. For comparison purposes, we have included results obtained using the Biersack universal planar potential [13], which is a refined version of the Thomas–Fermi potential, more frequently used in low-energy stopping power studies [14].

The basic principle of planar channelling and the various types of potential used in this comparative study are discussed in section 2. In section 3, CDR analysis using a numerical program is outlined. In section 4 we present results obtained using the shell and Biersack's universal potentials and compare them with the Moliere planar potential; we also give a discussion of these results.

2. Planar channelling in SLS and potentials used in the calculations

2.1. Potentials

The well known Moliere form of the Thomas–Fermi potential and the Biersack universal interatomic potential have similar general forms, and can be represented as [4, 13]

$$V(R) = \frac{Z_1 Z_2 e^2}{R} \sum_{i=1}^{g} a_i \exp(-b_i R) \tag{1}$$

where $g = 3$ for the Moliere potential and $g = 4$ for the Biersack universal potential. Here Z_1 and Z_2 are the atomic numbers of projectile and target atoms (SLS) respectively and e is the electronic charge. For the Moliere potential, $V(R) = V_M(R)$ and the relevant six fitting constants are given by $a_1 = a_{1M} = 0.35$; $a_2 = a_{2M} = 0.55$; $a_3 = a_{3M} = 0.1$; $b_1 = b_{1M} = 0.3/a_T$; $b_2 = b_{2M} = 1.2/a_T$; $b_3 = b_{3M} = 6.0/a_T$. For Biersack's universal potential $V(R) = V_U(R)$ and the relevant eight fitting constants are given by $a_1 = a_{1U} = 0.1818$; $a_2 = a_{2U} = 0.5099$; $a_3 = a_{3U} = 0.2802$; $a_4 = a_{4U} = 0.028\,17$; $b_1 = b_{1U} = 3.2/a_T$; $b_2 = b_{2U} = 0.9423/a_T$; $b_3 = b_{3U} = 0.4029/a_T$; $b_4 = b_{4U} = 0.2016/a_T$, where a_T is the Thomas–Fermi screening radius and is given by

$$a_T = \frac{0.8853 a_0}{(Z_1^{2/3} + Z_2^{2/3})^{1/2}} \tag{2}$$

with a_0 the Bohr radius.

The corresponding planar continuum potential due to a single plane is derived using the *continuum approximation* [4] (i.e. *averaging the interatomic potential over the plane*) and is given by [4, 10]

$$Y_M(y) = 2\pi N d_p \int r V \sqrt{r^2 + y^2}\, \mathrm{d}r = 2\pi N d_p Z_1 Z_2 e^2 \sum_{i=1}^{g} a_i \frac{\mathrm{e}^{-b_i y}}{b_i} \tag{3}$$

where N is the bulk density of atoms in the crystal, d_p is the interplanar distance and y is the distance measured from the plane.

The shell interatomic potential is based on spherically symmetric charge densities, which are evaluated using Slater orbitals with optimized orbital exponents given by Clementi and Raimondi [15]. This can be written in terms of individual shells as

$$V_S(R) = \frac{Z_1 e^2}{R} \sum_j \frac{\omega_j}{2n_j} e^{-2\xi_j R} \sum_{k=1}^{2n_j} \frac{k}{(2n_j - k)!} (2\xi_j R)^{2n_j - k} \tag{4}$$

where n_j is the principal quantum number, ω_j is the occupation number of the jth shell and ξ_j is the optimized orbital exponent. The corresponding shell planar potential is given by

$$Y_S(y) = 2\pi N d_p Z_1 e^2 \sum_j \frac{\omega_j}{2n_j} \sum_{k=1}^{2n_j} k(2\xi_j)^{2n_j - k} \sum_{m=0}^{2n_j - k} e^{-2\xi_j y} \frac{y^m}{m!(2\xi_j)^{2n_j - k - m + 1}}. \tag{5}$$

The average continuum potential due to two planes on either side of a channel is given by

$$U(x) = Y(\tfrac{1}{2}d_p + x) + Y(\tfrac{1}{2}d_p - x) - 2Y(\tfrac{1}{2}d_p) \tag{6}$$

where $Y(x)$ is the planar potential due to a single plane (equations (3) and (5)) and x is the transverse displacement of the channelled particle and is measured from the midpoints between the planes.

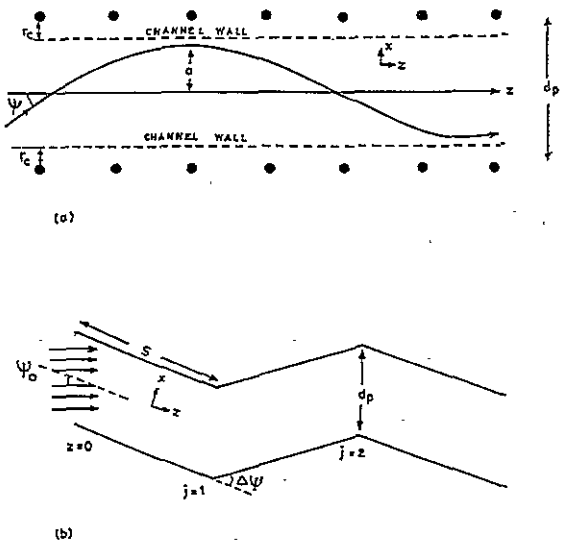

Figure 1. (*a*) Trajectory of a planar channelled particle. d_p is the interplanar spacing, r_c is the minimum impact parameter for channelling, ψ is the incident angle and a is the amplitude of the motion of a channelled particle. (*b*) Schematic diagram of a (110) planar channel of a strained layer superlattice. $\Delta\psi$ is the tilt angle, and s is the path length per layer of the SLS.

2.2. *Planar channelling in SLS*

The equation of motion for a SLS is given by

$$\frac{d^2x}{dz^2} + \frac{1}{2E_z}\frac{d}{dx}U(x) = \sum_{j=1}^{n}(-1)^j \Delta\psi\, \delta(z - js). \tag{7}$$

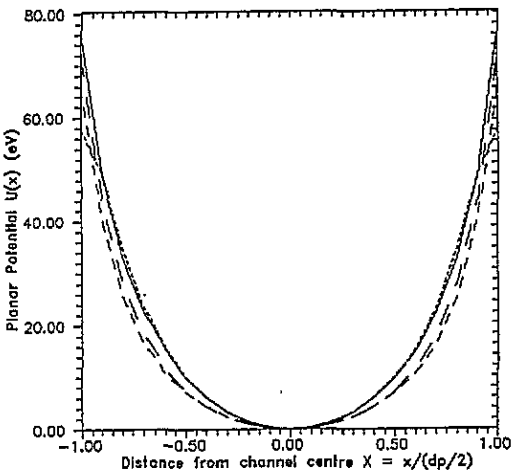

Figure 2. The Moliere (full curve), shell (dotted curve) and Biersack universal (broken curves) planar potentials for channelling of 1.2 MeV ^{4}He ions incident along the (110) plane of $GaAs_xP_{1-x}/GaP$ with $x = 0.075$.

(For a perfect single crystal, the right-hand side of the above equation will be zero.) In this equation x and z are the transverse and longitudinal displacements of channelled particles respectively. See figure 1. $U(x)$ is the averaged continuum planar potential, E_z is the longitudinal energy, and is almost equal to the incident energy E (i.e. $E_z = E$). s is the path length per layer; $\Delta\psi$ is the tilt angle as a result of elastic accommodation of strain, and is a direct measurement of strain in SLS.

Integrating the equation from js^- to js^+ gives

$$\psi(js^+) - \psi(js^-) = (-1)^j \Delta\psi. \tag{8}$$

3. Catastrophic dechannelling resonance

The main consequence of catastrophic dechannelling resonance (CDR) is that a large fraction of planar channelled particles is simultaneously focused onto the channel wall under these resonance conditions [6]. Maximum dechannelling occurs in this case. The CDR condition is satisfied experimentally by changing the beam energy until the effective wavelength matches the superlattice period ($\lambda = 2s$) as shown in figure 1. The effective wavelength of planar channelled particle motion can be experimentally determined from the oscillations in the backscattered yield as a function of a depth [7].

We have studied the depth and angular dependence of CDR as a function of incident angle (ψ_0), strain tilt angle ($\Delta\psi$) and minimum impact parameter (r_c). The minimum impact parameter r_c defines the cut-off distance for a channelled trajectory, and if a particle approaches a plane within a distance r_c of that plane, it is considered to be dechannelled. For each case, the continuum planar potentials discussed in the previous section were used and the results compared with experimental data, as discussed in the next section.

The trajectory of a planar channelled particle is simulated numerically by integrating equation (7) for each incident angle (ψ_0) and initial longitudinal displacement (z_0). The trajectory calculations were carried out for 200 incident particles spaced uniformly between the planes (i.e. varying the initial transverse displacement x_0 from $-d_p/2$ to $+d_p/2$). When a particle crosses the first interface ($z = s, j = 1$) there should be a change in ψ by an amount equal to $-\Delta\psi$. At the second interface ($z = 2s, j = 2$), this amount should be

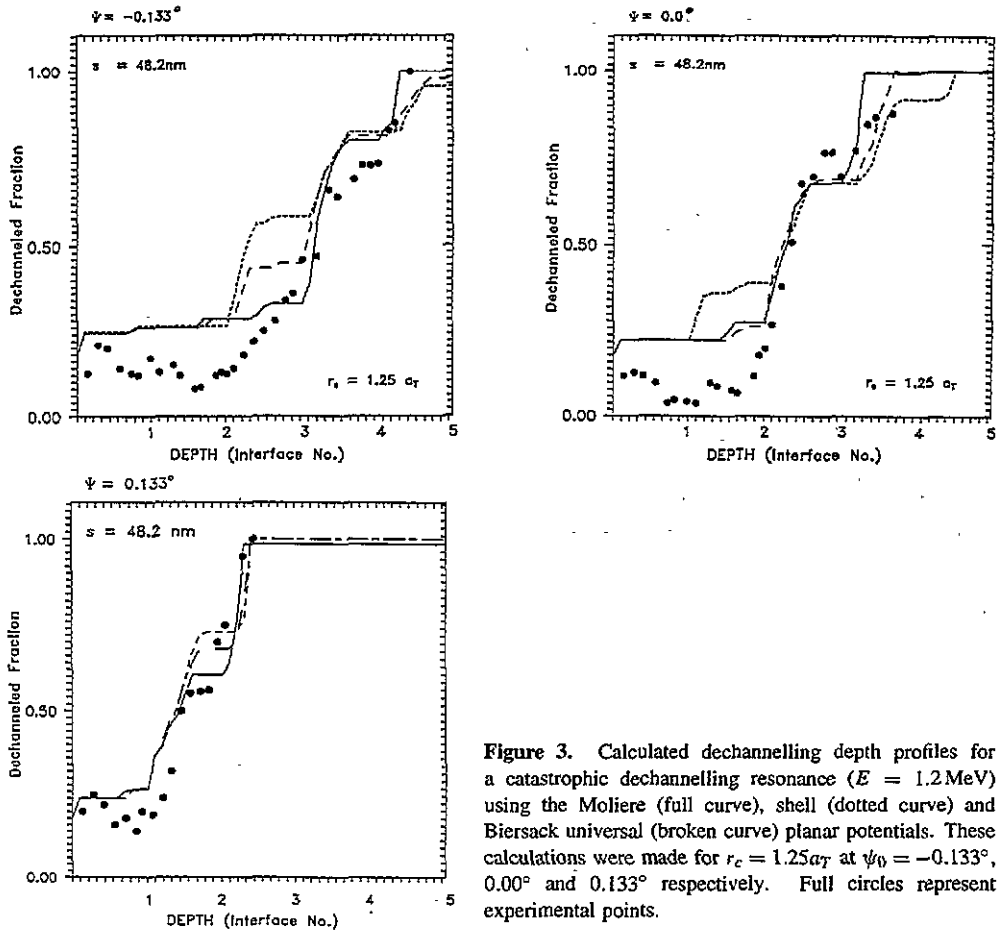

Figure 3. Calculated dechannelling depth profiles for a catastrophic dechannelling resonance ($E = 1.2$ MeV) using the Moliere (full curve), shell (dotted curve) and Biersack universal (broken curve) planar potentials. These calculations were made for $r_c = 1.25a_T$ at $\psi_0 = -0.133°$, 0.00° and 0.133° respectively. Full circles represent experimental points.

$+\Delta\psi$ because of opposite tilt. We have used this criterion for checking the program for various values of $\Delta\psi$ and ψ. All numerical calculations were carried out on a MicroVax II system with the help of the IMSL Math/Library™.

We calculated the dechannelling profile of 1.2 MeV ^{4}He particles in $GaAs_{0.09}P_{0.91}/GaP$ ($s = 48.2$ nm, layer thickness = 34 nm) for various incident angles ($\psi_0 = -0.133°$, 0.0°, 0.133°), tilt angles ($\Delta\psi = 0.143°$, 0.153°, 0.163°) and minimum impact parameters ($r_c = 1.15a_T$, $1.25a_T$ and $1.13a_T$) respectively. This particle energy corresponds to resonance conditions discussed above. Results are discussed in the next section.

4. Results and discussion

In figure 2, the Moliere, shell and Biersack universal average planar potentials are plotted as a function of distance from the centre of the channel. The shell potential gives a slightly smaller value near the planes compared to the Moliere and Biersack planar potentials. This implies that the dechannelling fraction calculated using the shell planar potential will be slightly greater than that given by the other two potentials.

There is a strong asymmetry in the incident angle dependence of CDR. When the incident angle is varied from $-\psi_0$ to ψ_0, the focusing of the channelled particles onto

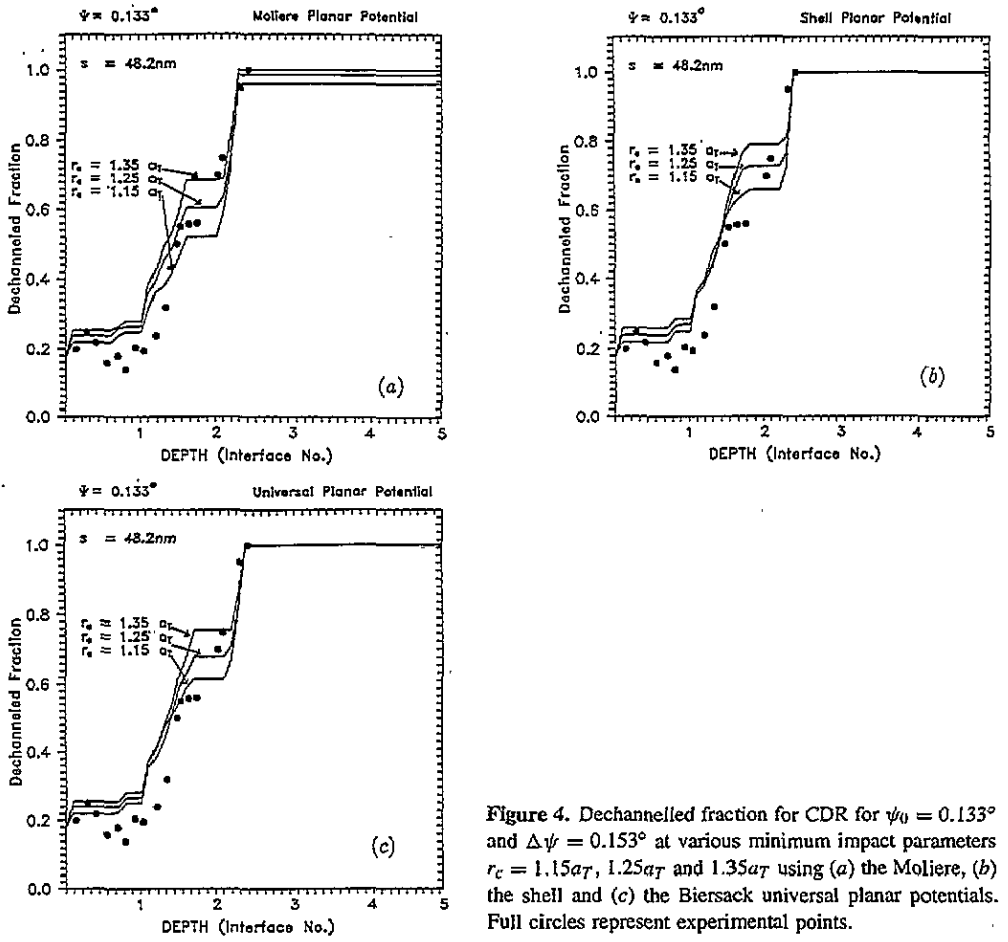

Figure 4. Dechannelled fraction for CDR for $\psi_0 = 0.133°$ and $\Delta\psi = 0.153°$ at various minimum impact parameters $r_c = 1.15a_T$, $1.25a_T$ and $1.35a_T$ using (*a*) the Moliere, (*b*) the shell and (*c*) the Biersack universal planar potentials. Full circles represent experimental points.

the channelling wall is advanced and the dechannelling depth is shifted to shallower depth (the angle ψ_0 ($-\psi_0$) is defined as towards (away) from the second-layer direction). This asymmetry in the incident angle can be understood from the phase plane model discussed elsewhere [3, 6]. This incident angle asymmetry is shown in figure 3, for $\psi_0 = -0.133°$, 0.00° and 0.133° respectively. When the angle is increased from −0.133° to 0.133°, the dechannelling at a given depth is increased. The dechannelling fractions calculated using the Moliere, shell and universal planar potentials compare well with experimental results. Specifically, the depth of the abrupt rise in dechannelling (a characteristic of CDR) matches well with the experimental points. When the angle is decreased, this marked increase in the dechannelling fraction diminishes.

For a larger minimum impact parameter r_c, only a few particles remain channelled because the effective channel width is decreased. The parameter $|d_p/2 - ba_T|$ determines the width of the channel , where b is a variable (1.15, 1.25 and 1.35 in the present case) and a_T is the Thomas–Fermi screening radius. So it is not surprising that dechannelling at a given depth is largest for the highest value of r_c, i.e. for $r_c = 1.35a_T$ (shown in figure 4). A similar situation exists for other values of tilt angle. For higher values of the tilt angle, the transverse energy acquired at the interface is large and that results in a sharp rise in the dechannelling fraction. This is shown in figure 5.

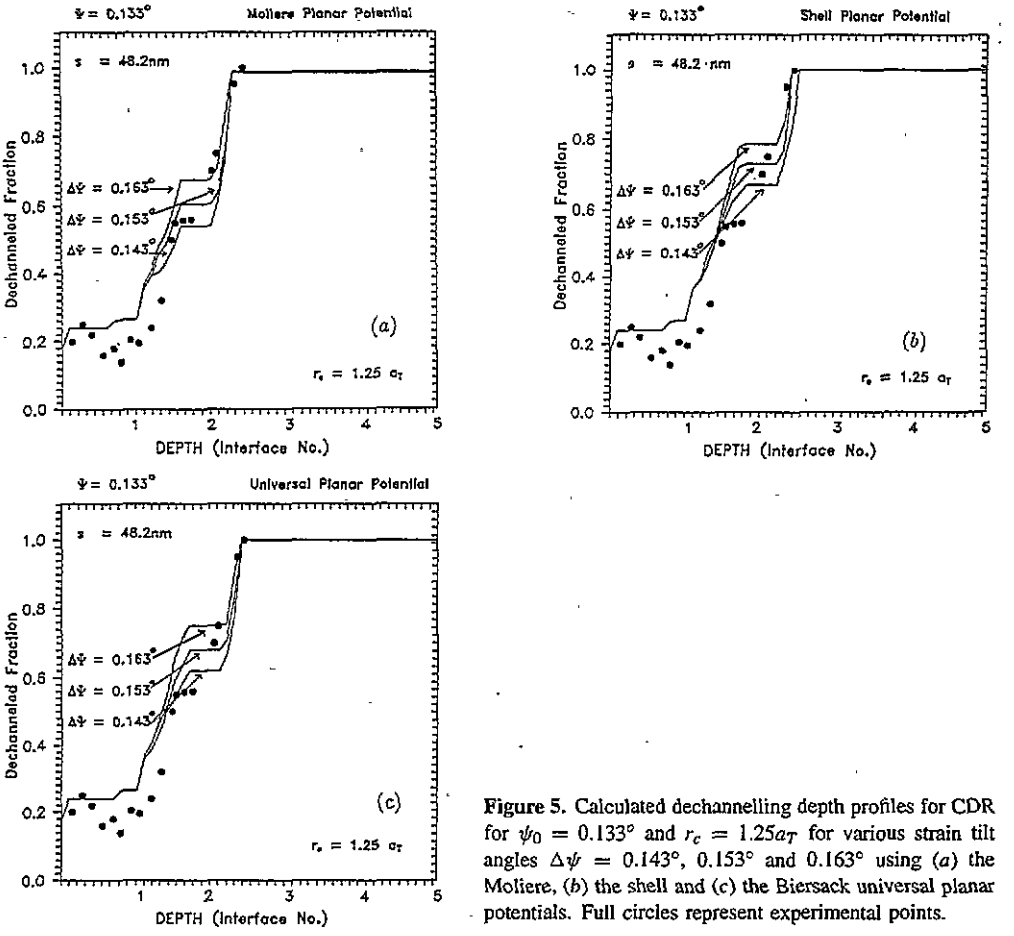

Figure 5. Calculated dechannelling depth profiles for CDR for $\psi_0 = 0.133°$ and $r_c = 1.25a_T$ for various strain tilt angles $\Delta\psi = 0.143°$, $0.153°$ and $0.163°$ using (*a*) the Moliere, (*b*) the shell and (c) the Biersack universal planar potentials. Full circles represent experimental points.

In conclusion, we have calculated the CDR dependence on various parameters using the Moliere, shell and Biersack universal planar potentials. The choice of the shell potential was due to its non-statistical nature, and the signature of the detailed atomic structure of target material is inherent in the shell model.

Acknowledgments

VHK thanks CSIR and IUC-DAEF for financial support.

References

[1] Chu W K, Ellison J A, Picraux S T, Biefeld R M and Osbourn G C 1994 *Phys. Rev. Lett.* **52** 125
[2] Pathak A P and Balagari P K J 1986 *Appl. Phys. Lett.* **48** 1075
[3] Picraux S T, Biefeld R M, Allen W R, Chu W K and Ellison J A 1988 *Phys. Rev.* B **38** 11 086
[4] Pathak A P 1982 *Radiat. Eff.* **61** 1
[5] Allen W R, Chu W K, Picraux S T, Biefeld R M and Ellison J A 1984 *Phys. Rev.* B **39** 3954
[6] Picraux S T, Allen W R, Biefeld R M, Ellison J A and Chu W K 1985 *Phys. Rev. Lett.* **54** 2355
[7] Ellison J A, Picraux S T, Allen W R and Chu W K 1988 *Phys. Rev.* B **37** 7290

[8] Chu W K, Allen W R, Picraux S T and Ellison J A 1990 *Phys. Rev.* B **42** 5923
[9] Slater J C 1960 *Quantum Theory of Matter* (New York: McGraw Hill) pp 317–26
[10] Hari kumar V and Pathak A P 1993 *Phys. Status Solidi* b **177** 269
[11] Hari kumar V and Pathak A P 1993 *J. Phys.: Condens. Matter* **5** 3163
[12] Hari kumar V and Pathak A P 1994 *Phys. Status Solidi* b **182** 51
[13] O'Conner D J and Biersack J P 1986 *Nucl. Instrum. Methods* B **15** 14
[14] Ziegler J F, Biersack J P and Littmark U 1984 *Stopping and Ranges of Ions in Matter* vol 1 (Oxford: Pergamon)
[15] Clementi E and Raimondi D L 1963 *J. Chem. Phys.* **38** 2686